INFLUENCE OF THE CURB SHAPE ON ROAD TRAFFIC AURALIZATION

Jonas Heck*, Hyeju Park*, Michael Vorländer

**These authors contributed equally to this work.*
Institute for Hearing Technology and Acoustics, RWTH Aachen University, Germany

This contribution has been accepted based on the submitted abstract. The submitted manuscript was not reviewed and is reproduced here without edits or corrections by the conference board. Neither the EAA nor the AAA take responsibility for its contents.

Preliminary document

Abstract

In outdoor sound propagation simulations, geometric modeling often focuses on large-scale features, while small roadside structures are neglected or simplified. For vehicle noise sources located close to the ground, roadside structures of similar height can modify the sound field and become perceptually relevant. Therefore, it can be important to consider in auralization, as it allows for listening to simulated scenarios by filtering an audio source signal through sound propagation effects. This contribution investigates the effects, different curb shapes introduce to the sound field emitted by road vehicles. The results show that curb geometry can have perceptual relevance for the auralization filters, which is discussed based on the psychoacoustic metrics loudness and sharpness. The effect size depends not only on curb shape but also on source–receiver configuration. Curb modeling may therefore improve perceptual realism for low-height traffic noise sources.

Keywords: *road traffic, auralization, noise, perception*

1. Introduction

Auralization promises to be a useful tool for traffic noise assessment, as it enables listeners to experience simulated traffic scenarios and evaluate them based on perception beyond conventional noise level metrics such as A-weighted sound pressure level. To achieve a perceptually convincing auralization, acoustic simulations must account for the sensitivity of human auditory perception, as even small deviations of the simulated sound field from a reference may be perceivable to listeners. Among the factors affecting simulation accuracy, the geometry of the target space plays a key role because it determines sound propagation paths.

In a number of road traffic auralization studies, outdoor sound propagation models such as Nord2000 [1] and Harmonoise [2] are employed to represent large-scale structures, considering terrain, street canyon, buildings, and noise barriers. For example, the LISTEN project developed a demonstrator based on Nord2000 and Harmonoise [3]. Viggen et al. proposed an urban auralization framework using Nord2000 [4]. Maillard et al. employed a noise evaluation software integrating a noise prediction tool with an auralization tool that applies the Harmonoise propagation model [5]. Some studies invested lower roadside structures, particularly low-height noise barriers as roadside noise mitigation measures [6], [7]. However, unlike such purpose-built acoustic structures, smaller existing roadside features, such as sidewalk steps, are generally not represented explicitly in simulation models.

This simplification may not always be justified in urban traffic scenarios. In Nord2000 [8] and Harmonoise [9], relevant noise source components are defined close to the ground, such that their height can be comparable to the height of a sidewalk step or curb. Consequently, these small roadside structures may modify the sound propagation from the sources to the receiver, thereby changing spectral characteristics of the received sound. Despite this potential difference, it remains unclear whether they lead to perceivable changes in auralized environments, and therefore whether these structures need to be explicitly represented in simulation models.

This study investigates the influence of curb geometry on road traffic auralization. A flat model without a sidewalk serves as the reference model for the simulation, against which sidewalk models with different curb shapes are compared. The simulation is based on the 2D Boundary Element Method (BEM) and delivers frequency responses for a number of static source-receiver configurations. They are used to filter a tyre-road noise. The result is analyzed by psychoa-

Corresponding author: *jonas.heck@akustik.rwth-aachen.de.*
Copyright: *©2026 Jonas Heck et al. This is an open-access article distributed under the terms of the Creative Commons Attribution 3.0 Unported License, which permits unrestricted use, distribution, and reproduction in any medium, provided the original author and source are credited.*

coustic metrics loudness and sharpness.

2. Methods

2.1. Geometry

The sidewalk modeling concept is illustrated in Fig. 1. While the sidewalk edge is located in the center, the roadway is located on the left side, whereas the sidewalk is located on the right side. For the **Flat Model (FM)**, the sidewalk thickness h_p was set to 0. For the simplified **Sidewalk Model (SM)**, a right-angle curb was used, with $h_p = 0.15\,\mathrm{m}$, consistent with the dimensions specified in DIN 483 [10].

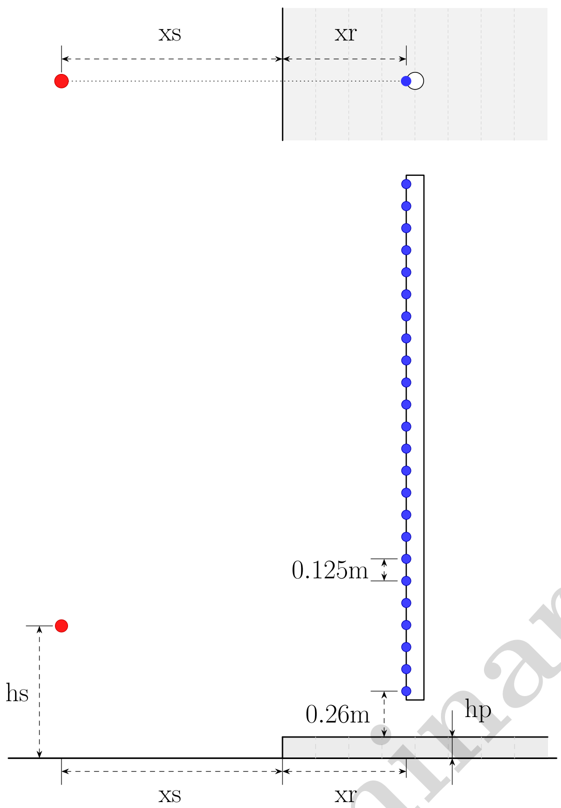

Figure 1: Simulation geometry: top view (top) and side view (bottom). The red point represents the source, the blue points represent the receivers.

The simulations were performed for different source positions determined based on the Harmonoise and Nord2000 prediction models. The vertical source position, h_s, depends on the vehicle noise component. The lateral source position was assumed to be at the wheel closest to the receiver, 1 m from the vehicle centerline [8], [9]. Furthermore, the horizontal source position in the simulation domain, x_s, accounted for a movement clearance of 0.25 m from the vehicle side, and an additional side safety clearance as specified in “Richtlinien für die Anlage von Stadtstraßen” (RASt06) [11]. The resulting source positions are summarized in Table 1. To isolate the effect of the presence of a sidewalk on the sound field and the perceived sound, the vehicle was modeled as an equivalent stationary source at the closest point of approach.

Table 1: Source positions

x_s (m)	h_s (m)
0.25, 0.50, 0.75, 1.25	0.01, 0.30, 0.75

The horizontal receiver position x_r was defined relative to the sidewalk width. According to RASt06, the sidewalk width for urban roads or local main streets is generally recommended to be 3.0 m [11]. Based on this recommendation, the receivers were assumed to be positioned at the center of the sidewalk, corresponding to 1.5 m from the sidewalk edge. As shown in Fig. 1, 24 receivers were arranged along the z-axis, starting at a height of 0.26 m above the sidewalk surface, with a spacing of 0.125 m.
To further investigate detailed curb shapes, two different curb types, namely the **High Curb (Hochbordstein, HB)** and **Flat Curb (Flachbordstein, FB)**, were considered based on DIN 483 [10], as shown in Fig. 2.

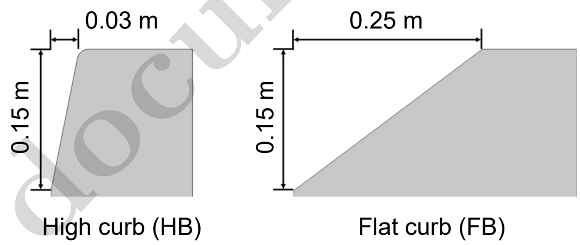

Figure 2: Different curb shapes

2.2. Numerical Setup

The acoustic field was simulated using a 2D BEM solver in COMSOL Multiphysics [12]. Since the sidewalk geometry was assumed to be approximately invariant along the road direction, the problem was considered suitable for 2D simulation.
The simulations were performed over the frequency range from 20 Hz to 10 kHz with a mixed frequency resolution:

- 1/12-octave spacing below 1.73 kHz and
- 100 Hz linear spacing above 1.73 kHz.

This resolution was chosen to keep sufficient detail at low frequencies while capturing narrow high-frequency features, such as notches, without unnecessary computational cost.
All the boundary surfaces were assumed to be acoustically rigid and were therefore modeled as a sound-hard boundary condition in COMSOL. The boundary mesh size was set based on $\lambda/6$, where λ denotes the acoustic wavelength at each simulated frequency. In addition, the minimum receiver height above the boundary surface $h_{\mathrm{r,min}}$ was considered to avoid near-singular integration errors for receivers close to, but not directly on, the surface. The final maximum mesh size was chosen according to

Preliminary document

$$h \leq \min\left(\frac{h_{\mathrm{r,min}}}{N}, \frac{\lambda}{6}\right), \quad (1)$$

where N was determined iteratively and empirically set to 7. This combined criterion was used to ensure sufficient accuracy of both the near-singular integration and the acoustic wavelength resolution, providing stable results especially at low frequencies, while keeping the computational effort reasonable.
Following the Harmonoise prediction model, the vehicle noise source was represented as a point source in the simulations. However, because 2D formulation assumes invariance in the out-of-plane direction, this source corresponds to an infinitely long line source in 3D and leads to a different geometrical spreading behavior from that of a 3D point source. To compensate for this difference, a correction factor was derived from the Green's functions of a 3D point source and a 2D line source,

$$C(r, k) = \sqrt{\pi k \frac{1[\mathrm{m}]}{2r}}, \quad (2)$$

where k is wavenumber and r denotes the distance between the source and the receiver positions. Accordingly, a cylindrical wave was implemented in COMSOL as a background sound field representing a line source. After the simulation the correction function in Eq. 2 was applied to the simulated sound pressure $p_{2\mathrm{D}}(r, k)$ to obtain the corresponding 3D point source result $p_{3\mathrm{D}}(r, k)$. Subsequently, $p_{3\mathrm{D}}$ was normalized by the sound pressure at a distance of 1 m for further post-processing and comparison.

2.3. Post-Processing

The signals for the psychoacoustic analysis were generated by convolving a source signal with the simulated transfer functions. As the BEM results were available only at a limited number of non-uniformly spaced frequency points, the transfer functions were reconstructed on a uniformly spaced, high-resolution frequency grid prior to the convolution. First, the magnitude response is interpolated using a cubic spline. Then, a minimum-phase response is derived from the interpolated magnitude response based on the Hilbert transform of the real-valued cepstrum and a linear phase term corresponding to the direct sound path is added. Finally, the interpolated magnitude response and the reconstructed phase response are combined to obtain the complete transfer function.
For the source signal, the spectral characteristics of road traffic noise, particularly those originating from the tyre-road contact of passenger cars, are considered. Tyre-road noise exhibits a broadband character, with the sound level gradually decreasing toward higher frequencies [9]. This overall tendency is similar to that of pink noise. Therefore, pink noise was used as the source signal in this study. The sound power level is selected based on the driving speed of passenger cars according to the Harmonoise prediction model and was set to 93 $\mathrm{dB_{SWL}}$ for constant driving speed of 50 km/h [13].

2.4. Psychoacoustic Metrics

To assess whether the differences between the FM and the different curb models may be perceptually relevant, psychoacoustic metrics were calculated from the generated audio signals. Loudness and sharpness were selected because they promise to capture perceptual characteristics of traffic noise.
Loudness N was calculated using the Zwicker method according to ISO 532-1 [14]. The relative loudness difference was calculated with respect to the loudness obtained for the reference model,

$$\Delta N_{\mathrm{rel}} = \frac{|N - N_{\mathrm{ref}}|}{N_{\mathrm{ref}}} \times 100\%, \quad (3)$$

where N_{ref} and N denote the loudness values of the reference model (FM) and target model, i.e. SM, HB, and FB, respectively. In this study, the just noticeable difference (JND) in loudness was assumed to be 5 % of the reference loudness, based on Weber's law [15]. Therefore, A threshold of $\Delta N_{\mathrm{rel}} \geq 5\,\%$ was used as the criterion for a potentially perceivable loudness difference.
Sharpness S was calculated according to Aures [16]. Since this model includes a loudness-dependent weighting, differences in loudness between FM and the other models do influence the calculated sharpness values. However, reported JNDs for sharpness are typically obtained under controlled conditions with constant loudness and according to DIN 45692 [17]. Accordingly, no JND was applied to sharpness; instead, sharpness was evaluated comparatively between the two models using the absolute difference

$$|\Delta S| = |S - S_{\mathrm{ref}}|, \quad (4)$$

where S_{ref} and S denote the sharpness values of the reference model (FM) and the other models, respectively.

3. Results

3.1. Sound Field in the Presence of a Sidewalk

Fig. 3 shows the frequency response of the FM, SM, HB and FB for each source height at the distance $x_s = 0.25$ m. For the results presented here, four receiver heights were selected: 0.26 m, 1.01 m, 1.76 m and 2.51 m.

3.1.1. Simplified Sidewalk Model

First, to investigate the influence of a sidewalk step on sound propagation, FM, shown as pink solid line, and SM, shown as blue solid line, are compared. The differences between FM and SM can be mainly observed in the interference pattern, particularly in the notch depths and their frequency locations. For $h_s = 0.01$ m, SM exhibits pronounced attenuation at high frequencies at $h_r = 0.26$ m. With increasing h_r, this attenuation becomes progressively weaker, and the SM response approaches that of FM. At $h_s = 0.3$ m the interference pattern of SM differs clearly from that

Preliminary document

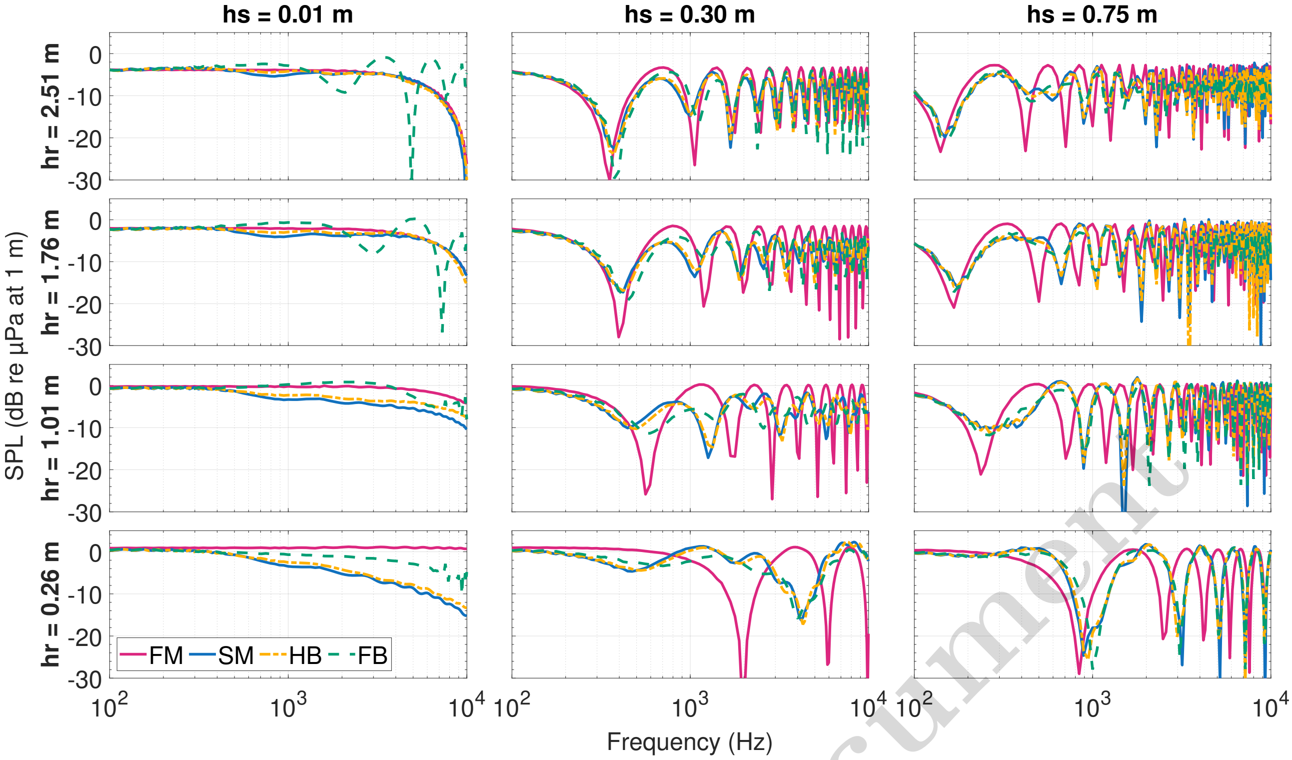

Figure 3: Comparison of frequency responses for FM and all curb shapes at $x_s = 0.25\,\text{m}$. Only four representative receiver heights, $h_r = 0.26\,\text{m}$, $1.01\,\text{m}$, $1.76\,\text{m}$ and $2.51\,\text{m}$, are shown for clarity.

Preliminary document

of FM at $h_r = 0.26\,\text{m}$, the notch locations approach those of FM as h_r increases, while the notch depths vary non-monotonically. For $h_s = 0.75\,\text{m}$, the SM notch depths slowly become shallower, but the notch locations do not converge as clearly to FM, particularly in the the mid-frequency range.

Although only results for $x_s = 0.25\,\text{m}$ are shown in Fig. 3, additional simulations were performed for larger x_s values, as listed in Table 1. Increasing x_s reduces the high-frequency attenuation in the SM responses and leads to close agreement with FM at lower h_r. For $h_s = 0.3\,\text{m}$, SM still shows a clearly different interference pattern from FM at the lowest h_r. However, compared with the case of $x_s = 0.25\,\text{m}$, the non-monotonic trend is shifted toward lower receiver heights and is confined to a narrower range of h_r. The same tendency is also found for $h_s = 0.75\,\text{m}$.

3.1.2. Realistic Curb Shapes

To examine the influence of more realistic curb shapes, the analysis is extended to the curbs introduced in Sec. 2.1. The following analysis focuses on SM, HB, and FB, shown as blue solid line, yellow dash-dotted line, and green dashed line, respectively.

The different curb shapes produce similar broadband trends, with the HB showing the closest agreement with the SM. This suggests that the simplified SM captures the overall spectral behavior of a realistic HB model reasonably well.

Differences from SM are most pronounced in the FB case, where deviations at high frequencies are noticeable. For $h_s = 0.01\,\text{m}$, FB shows less attenuation than SM and HB at lower h_r, while exhibiting a different interference pattern as h_r increases. For $h_s = 0.3\,\text{m}$, the remaining differences are mainly observed as slight shifts in the notch locations. For $h_s = 0.75\,\text{m}$, FB exhibits the weakest interference pattern, characterized by reduced spectral fluctuations at higher h_r.

3.2. Perceptual Implications

Since the frequency responses showed that the sidewalk step alters the sound field, the following analysis examines whether these changes are perceptually relevant. Based on the good agreement between SM and HB observed in Section 3.1.2, the psychoacoustic analysis compares HB and FB with FM.

3.2.1. Loudness

Fig. 4a and Fig. 4c show the relative loudness differences between HB and FM, and between FB and FM, respectively. The source–receiver configurations with $\Delta N_{\text{rel}} < 5\,\%$ are shown in gray, while those with $\Delta N_{\text{rel}} \geq 5\,\%$ are represented using a heatmap. Overall, the results indicate that curbs can produce perceivable differences in loudness, depending on the source–receiver configuration.

In Fig. 4a, the potentially perceivable loudness region covers a broad range of receiver heights at $x_s = 0.25\,\text{m}$, with its location varying with source height. Configurations exceeding the JND criterion are mainly found at lower receiver heights for $h_s = 0.01\,\text{m}$, at intermediate heights for $h_s = 0.3\,\text{m}$, and at higher receiver positions for $h_s = 0.75\,\text{m}$. With increasing x_s, regions

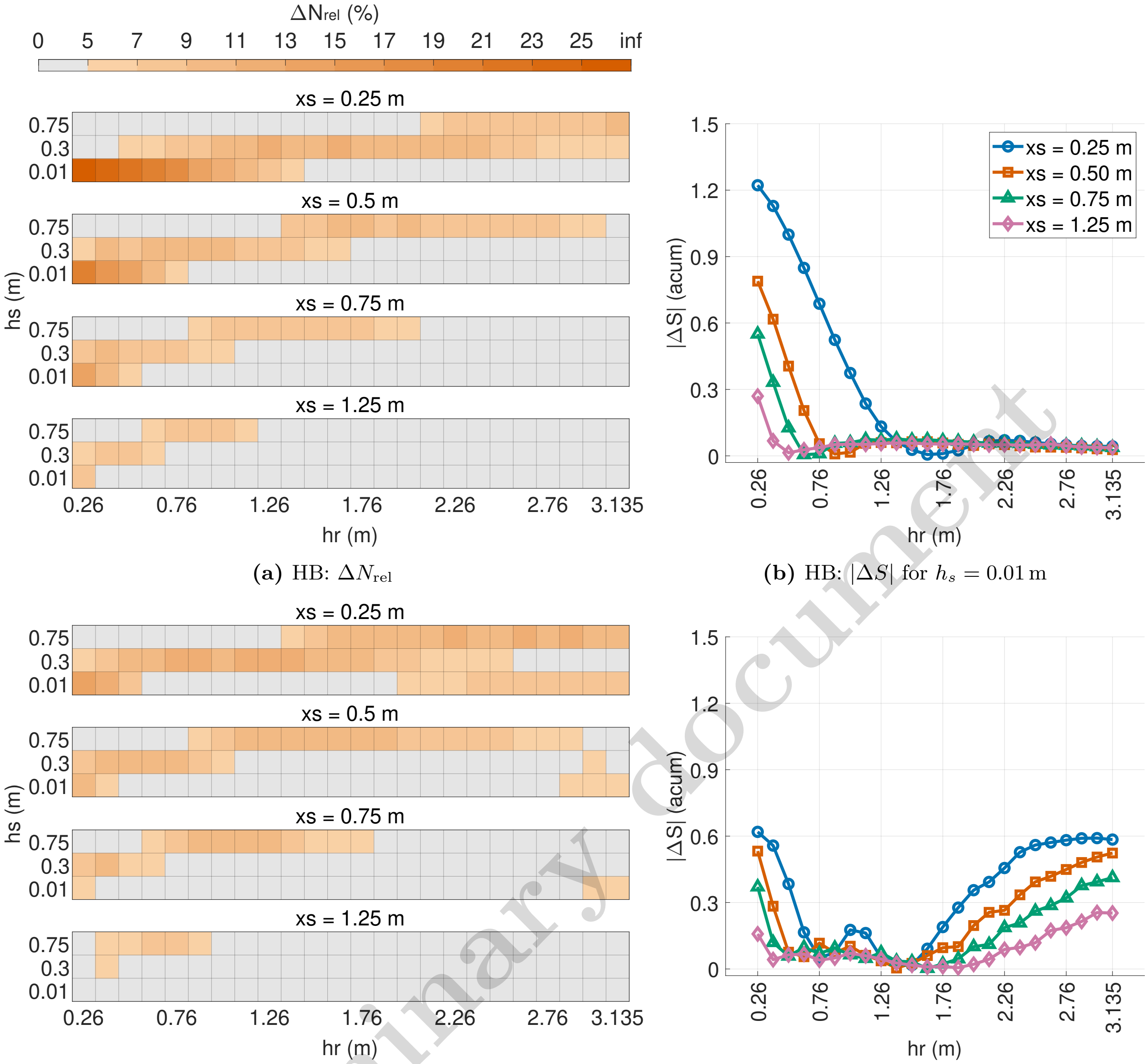

(a) HB: ΔN_{rel}

(b) HB: $|\Delta S|$ for $h_s = 0.01\,\text{m}$

(c) FB: ΔN_{rel}

(d) FB: $|\Delta S|$ for $h_s = 0.01\,\text{m}$

Figure 4: Relative loudness difference ΔN_{rel} (left) and absolute sharpness difference $|\Delta S|$ for $h_s = 0.01\,\text{m}$ (right) with respect to FM, for HB (top) and FB (bottom).

Preliminary document

above the JND become smaller and shift toward lower receiver height.

A similar overall trend is shown for the FB in Fig. 4c, but with a different perceivable loudness pattern for $h_s = 0.01\,\text{m}$. At this source height, the potentially perceivable loudness region is divided into two separate regions located at lower and higher receiver heights.

3.2.2. Sharpness

Fig. 4b and Fig. 4d show the absolute sharpness differences between HB and FM, as well as between FB and FM, for $h_s = 0.01\,\text{m}$. The most pronounced sharpness differences and the clearest trends can be observed for this source height. For the other source heights, $|\Delta S|$ remains below approximately 0.3 acum and does not exhibit similarly distinct patterns.

In Fig. 4b, $|\Delta S|$ of HB is largest at lower receiver heights and decreases rapidly with increasing h_r. Largest values occur for the smallest source distance from the sidewalk edge, $x_s = 0.25\,\text{m}$. For a given receiver height, $|\Delta S|$ generally decreases as x_s increases, and noticeable differences become confined to lower receiver heights.

In Fig. 4d, $|\Delta S|$ of FB is relatively large at lower receiver heights, decreases to a minimum at intermediate heights, and then increases again toward higher receiver heights. This trend is observed for all source distances, although the magnitude of $|\Delta S|$ progressively decreases as x_s increases.

4. Conclusion

This study examined the acoustic and perceptual effects of sidewalk curb geometry by comparing a flat model with simplified and realistic curb shapes. Depending on the source height, the elevated sidewalk either blocks the direct and reflected sound paths, leading to high-frequency attenuation or alters the reflection path, thereby modifying the interference pattern. Among the investigated curb shapes, HB exhibited the closest agreement with SM, suggesting that the simplified right-angle curb provides a reasonable approximation of conventional high curbs. In contrast, the larger deviations observed for FB, mainly at higher frequencies, indicate that although the presence of a curb is the dominant factor, local curb geometry can further modify the interference pattern.

The loudness and sharpness analysis further demonstrated that these acoustic differences can become perceptually relevant. For a range of source-receiver combinations, loudness differences appear to be well above commonly employed JNDs. HB and FB exhibited different patterns for loudness and sharpness relative to FM, consistent with their distinct frequency responses.

Accordingly, curb modeling supposably improves the perceptual realism of outdoor auralization for a certain range curb shape and source-receiver configuration, while it might not be necessary for every case. The findings suggest that, for example, a standing person close to the road experiences the differences for relatively high sound sources only. If the person is further away, then the differences become perceivable already at lower source heights.

In future work, listening experiments will be conducted to determine whether the predicted differences are actually perceivable and to identify perceptual dimensions, beyond loudness and sharpness, that contribute to the perception of differences between small-scale roadside structures such as sidewalk models. Furthermore, this study considered only tyre noise and ignored propulsion noise, looking at only one source position at a time. Though, according to Nord2000 and Harmonoise, both sources are emitted simultaneously [8], [9], which should be taken into consideration.

References

[1] B. Plovsing, "Nord2000. comprehensive outdoor sound propagation model. part 1: Propagation in an atmosphere without significant refraction," Danish Electronics, Light & Acoustics, Report AV 1849/00, 2006.

[2] E. Salomons, D. van Maercke, J. Defrance, and F. de Roo, "The harmonoise sound propagation model," *Acta Acustica United With Acustica*, vol. 97, no. 1, pp. 62–74, 2011.

[3] M. E. Nilsson, J. Forssén, P. Lundén, A. Peplow, and B. Hellström, "Listen auralization of urban soundscapes," Final Report to the Knowledge Foundation, 2011.

[4] E. M. Viggen, A. Solvang, J. Vennerød, and H. Olsen, "Development of an outdoor auralisation prototype with 3D sound reproduction," in *Proc. of the 18th International Conference on Digital Audio Effects*, Trondheim, Norway, 2015, pp. 415–422.

[5] J. Maillard and J. Jagla, "Real time auralization of non-stationary traffic noise - quantitative and perceptual validation in an urban street," in *Proc. of the AIA-DAGA Conference on Acoustics*, Merano, Italy, 2013, pp. 110–113.

[6] P. Thomas et al., "Auralisation of a car pass-by behind a low finite-length vegetated noise barrier," in *Proc. of the 9th European Conference on Noise Control*, Prague, Czech Republic, 2012, pp. 932–937.

[7] A. J. Torija and I. H. Flindell, "Listening laboratory study of low height roadside noise barrier performance compared against in-situ field data," *Building and Environment*, vol. 81, pp. 216–225, 2014.

[8] H. G. Jonasson, "Acoustic source modelling of nordic road vehicles," SP Swedish National Testing and Research Institute, SP Report 2006:12, 2006.

[9] H. G. Jonasson, "Acoustical source modelling of road vehicles," *Acta Acustica United With Acustica*, vol. 93, no. 2, pp. 173–184, 2007.

[10] DIN, "Concrete kerb units - shapes, dimensions, marking," DIN German Institute for Standardization, DIN 483:2005, 2005.

[11] FGSV, "Richtlinien für die Anlage von Stadtstraßen: RASt06," Forschungsgesellschaft für Straßen- und Verkehrswesen, Tech. Regulations, 2006.

[12] COMSOL AB, *COMSOL Multiphysics®*, version 6.3. [Online]. Available: `www.comsol.com`

[13] C. G. Dreier, "Virtual acoustics: Synthesis of traffic sound sources," Ph.D. dissertation, RWTH Aachen University, 2025.

[14] ISO, "Acoustics – methods for calculating loudness – part 1: Zwicker method," International Organization for Standardization, ISO 532-1:2017, 2017.

[15] G. A. Miller, "Sensitivity to changes in the intensity of white noise and its relation to masking and loudness," *The Journal of the Acoustical Society of America*, vol. 19, no. 4, pp. 609–619, 1947.

[16] W. Aures, "Der sensorische Wohlklang als Funktion psychoakustischer Empfindungsgrößen," *Acta Acustica*, vol. 58, no. 5, pp. 282–290, 1985.

[17] DIN, "Measurement technique for the simulation of the auditory sensation of sharpness," DIN German Institute for Standardization, DIN 45692:2009, 2009.

Preliminary document